JOURNAL OF RAMAN SPECTROSCOPY
J. Raman Spectrosc. **31**, 365–371 (2000)

Raman difference spectroscopic studies of dithiobenzoyl substrate and product analogs binding to the enzyme dehalogenase: π-electron polarization is prevented by the C=O to C=S substitution

Jian Dong,[1] Lusong Luo,[2] Po-Huang Liang,[2] Debra Dunaway-Mariano[2] and Paul R. Carey[1]*
[1] Department of Biochemistry, Case Western Reserve University, Cleveland, Ohio 44106-4935, USA
[2] Department of Chemistry, University of New Mexico, Albuquerque, New Mexico 87131, USA

The enzyme 4-chlorobenzoyl coenzyme A (CoA) dehalogenase catalyzes the transformation of 4-chlorobenzoyl-CoA to 4-hydroxybenzoyl-CoA. High-quality Raman spectra of substrate or product or their analogs in the enzyme's active site can be obtained using Raman difference spectroscopy. Here, data are presented for the substrate and product analog, 4-chlorobenzoyldithio-CoA and 4-hydroxybenzoyldithio-CoA, respectively, where the benzoyl C=O group has been replaced by C=S. The rationale behind this substitution is to explore the consequences of perturbing enzyme active site–ligand C=O interactions. Interpretation of the Raman data for the complexes was placed on a firm footing by undertaking density functional theory calculations on the model compounds *S*-ethyl 4-chlorobenzoate dithioester and *S*-ethyl 4-hydroxybenzoate dithioester. Based on the calculations and on data for the CoA moiety, essentially all the Raman bands in the spectra of the substrate and product dithio analogs could be assigned with confidence. The calculations show that the dithioester phenyl moiety is non-planar with the C=S bond typically being twisted 30° out of the plane of the phenyl ring. The Raman difference data for the dehalogenase bound dithio-based substrate and product show that only minor spectral changes occur upon binding and this indicates that the conformation about the dithioester bonds is essentially unchanged by binding. The results for the product analog are in strong contrast to those for the complex involving the natural product, 4-hydroxybenzoyl-CoA, where binding brings about a complete rearrangement of the benzoyl's normal modes. The reorganization is due to a marked polarization of the benzoyl's π-electrons, which, in turn, is brought about by electron pulling forces acting at the carbonyl and electron pushing forces near the benzoyl 4-position in the active site. However, π-electron polarization, and the accompanying normal mode rearrangement, do not happen for the dithio analog because the C=S substituted group does not transmit the electron pulling forces, that act on the C=O in the natural substrate, to the phenyl ring. The spectroscopic results explain why the dithio-based substrate reacts with dehalogenase 200 times more slowly than the thiolester substrate. For the latter, electron pull at the C=O is used to deplete electron density at the benzoyl's 4-position and to facilitate the substitution of the 4-Cl atom by the 4-OH group.

INTRODUCTION

Remarkably, during the past few decades, soil-dwelling bacteria have developed the ability to degrade environmentally harmful chlorinated hydrocarbons. They achieve this by producing novel enzymes that use the chlorinated hydrocarbons as substrates. In the present work we are concerned with a dehalogenase enzyme that acts in concert with two other bacterium-produced enzymes to convert *p*-chlorobenzoic acid to the benign *p*-hydroxybenzoic acid. The dehalogenase carries out the chemically difficult reaction shown in Scheme 1, where CoA is the co-factor coenzyme A. This reaction has been studied in detail by biochemical methodologies[1–3] and the structure of the product *p*-hydroxybenzoyl-CoA (4-HBA-CoA) bound to the dehalogenase enzyme has been derived using x-ray crystallography.[4]

These approaches have led to a broad appreciation of the mechanism. Critical details on the chemical mechanism of this reaction have been supplied by Raman spectroscopy.[5,6] Taking advantage of recent gains in sensitivity,[7] high-quality Raman difference data have been obtained for a large number of complexes involving dehalogenase, or mutant forms of the enzyme, and different substrate, substrate analog or product molecules.[8,9] One early finding of the Raman studies concerned the enzyme–product complex.[5] The Raman difference spectra showed that the π-electrons in the bound substrate undergo major reorganization with the phenyl ring losing its aromatic character and becoming quinonoid-like. That is, the bound structure has large contributions from canonical form **II** (Scheme 2).

* Correspondence to: P. R. Carey, Department of Biochemistry, Case Western Reserve University, Cleveland, Ohio 44106-4935, USA; e-mail: carey@biochemistry.cwru.edu
Contract/grant sponsor: NIH; Contract/grant number: GM-54072; Contract/grant number: GM-28688.

Received 27 July 1999
Accepted 14 October 1999

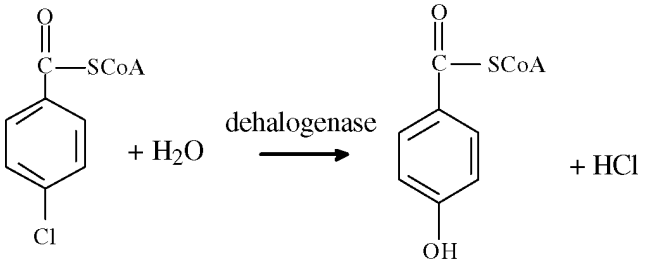

Scheme 1

The electron cloud in form **II** is highly polarized and the enzyme groups that bring this about have been identified in the x-ray structure. Strong electron pull at the benzoyl C═O group is provided by two hydrogen bonds from protein backbone NH groups and the partial positive charge from an α-helix dipole (represented by positive signs in Scheme 2). Electron push is provided by a negatively charged aspartate side-chain (Asp145) placed near the *para* position of the ring. The polarizing forces are amplified by the effect of a sheath of aromatic side-chains around the benzoyl ring in the active site; these provide a low dielectric environment. In the present work, we set out to explore the effect of modifying the interactions between the active site and the benzoyl C═O group. This was undertaken by making a single atom change, replacing the C═O by a C═S group in the substrate molecule. We show that this simple change has a profound effect on the properties of the bound product and that these differences can be used to explain why the C═S substituted compound 4-chlorobenzoyldithio-CoA is such a poor substrate.

EXPERIMENTAL

Sample preparation

Pseudomonas sp. strain CBS3 4-chlorobenzoyl-CoA dehalogenase was purified from an *E. coli* expression system,[2] according to the previous report by Liang *et al.*[3] 4-Chlorobenzoyldithio-CoA (4-CBA-dithio-CoA) was prepared by the use of Lawesson's reagent as described by Liang.[10] Briefly, 4-chlorobenzoyl chloride was reacted with thiophenol (1 : 1 molar ratio) to generate *S*-phenyl-4-chlorobenzoyl thiolester. The latter was refluxed with Lawesson's reagent [2,4-bis(4-methoxyphenyl)-1,3-dithia-2,4-diphosphetane-2,4-disulfide], yielding *S*-phenyl 4-chlorobenzoate dithioester, which was then reacted with CoA in buffered aqueous methanol solvent to generate desired CoA adduct. EI-MS, HR-MS, ^{13}C NMR and ^{1}H NMR technique were utilized to characterize the intermediate and product. 4-Hydroxybenzoyldithio-CoA (4-HBA-dithio-CoA) was generated by incubation of 4-CBA-dithio-CoA in wild-type enzyme ([E] : [S] = 1 : 20) for 6 h and filtration with Amicon-10 concentrators.

Instrumentation

The normal (non-resonant) Raman spectra were obtained using 647.1 nm laser excitation from an Innova 400 krypton laser system (Coherent) and a back-illuminated CCD detector (Model 1024EHRB/1, Princeton Instruments) operating at 183 K. Details of the spectrometer have been described previously.[7] In brief, a Holospec f/1.4 axial transmission spectrometer (Kaiser Optical Systems) equipped with a holographic Supernotch-Plus filter and a transmissive holographic grating was employed as a single monochromator (0.085 m). Enzyme samples contained in cuvettes were 60 μl in volume and buffered with 50 mM Tris–HCl at pH 7.5. 4-CBA-dithio-CoA was added at concentrations lower than that of the active site of enzyme, and the data were collected immediately after the complex had been made, under a laser power of ~850 mW. The Raman spectrum of the buffer was subtracted from that of the ligand in buffer (giving the spectrum of free ligand), while the spectrum of the enzyme in buffer was subtracted from that of the enzyme–ligand complex in buffer (giving the spectrum of the enzyme-bound ligand). During experiments, the concentration of

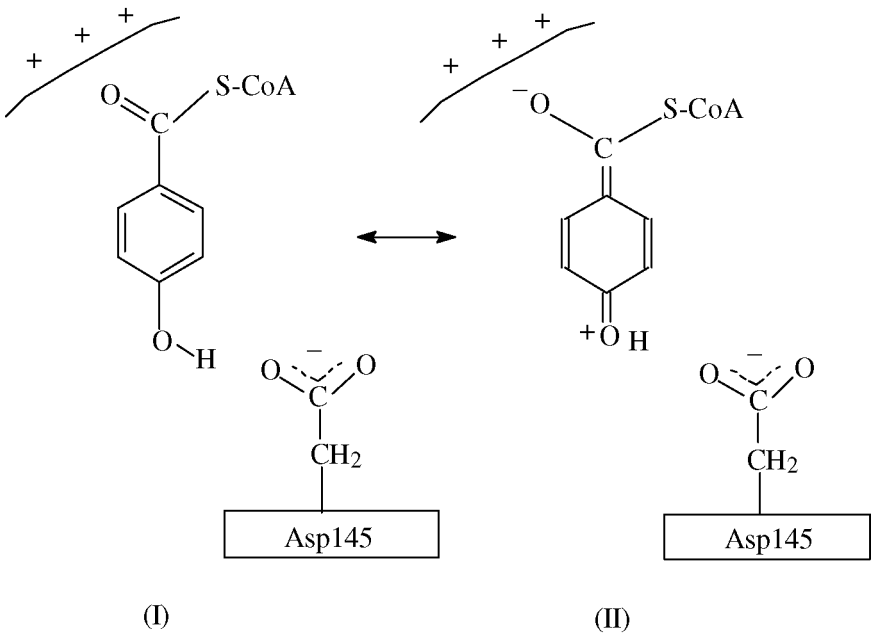

Scheme 2

the 'free' enzyme ought to be made identical with the enzyme concentration in the complex to circumvent the manipulation of the subtraction factor. Several factors contribute to the stability of our Raman instrumentation and assist in undertaking accurate differential experiments.

Neither the sample arrangement nor any optical component (lenses or grating) inside the spectrograph moves during data acquisition. This is important to ensure that the images of the two parent spectral signals do not undergo a displacement with respect to each other. It has been found that the Raman spectrum of the substrate ligand bound to the protein produces a signal intensity of ~110 000 counts min^{-1} for the 7a′ modes near 1237 cm^{-1} in the first minute, whereas the protein has a background level of only about 150 000 counts min^{-1}. Another favorable factor for the Raman difference experiments in this study is that the noise amplitude for the pure protein is only ~2000 counts min^{-1} under the same laser power condition. This is considerably smaller than the Raman signal intensities for a bound ligand, e.g. 110 000 counts min^{-1} for the 7a′ modes near 1237 cm^{-1} and 160 000 counts min^{-1} for 8a,b mode at 1585 cm^{-1}. This means that signal-to-noise ratios (S/N) of 55–80 can be achieved for the strong peaks of bound ligands, significantly greater than the normal condition to identify a peak (S/N ≈ 3).

Vibrational analysis

Harmonic wavenumber calculations on *S*-ethyl 4-chlorobenzoate dithioester and *S*-ethyl 4-hydroxybenzoate dithioester were carried out with the Gaussian 94 package[11] on a T90 vector processor at the Ohio Supercomputer Center (Columbus, OH, USA) or an SGI workstation in this laboratory. The geometry of each molecule was fully relaxed without any constraint and completely optimized with respect to all geometric parameters at the appropriate level of theory. A density functional theory (DFT) variant with Becke's three-parameter hybrid method using the Lee–Yang–Parr correlation functional (B3LYP)[12] was employed, in conjunction with a diffusion function augmented basis set of 6–31+G(d) to give normal modes. Meanwhile, the Hartree–Fock (HF) method with the same basis set was applied, producing Raman activities and nearly the same normal modes as those from the DFT method. Confirmatory geometries were obtained by both the HF and DFT methods, indicating consistent structures of the dithioester compounds. The calculated wavenumbers at the B3LYP/6–31+G(d) level were converted by a single scaling factor (0.9850) through a least-squares approach, mainly to correct for the anharmonicity. Normal modes related to ring vibrations (in Wilson's notation) are described according to Colthup *et al.*[13] and Dollish *et al.*[14] Only the *anti*-conformer of the *S*-ethyl group (rotation about the S—C bond in the C—S—CH_2—CH_3 moiety) was needed for the calculation, since the *gauche* conformers actually produce little difference in the wavenumbers associated with the ring and the dithioester groups.

RESULTS AND DISCUSSION

Conformations of *S*-ethyl 4-chlorobenzoate dithioester and *S*-ethyl 4-hydroxybenzoate dithioester

The conformations of these compounds, derived from DFT calculations, are illustrated in Fig. 1 [*ab initio* calculations at the HF/6–31+G(d) level produced similar conformational results]. Table 1 lists some of the important structural parameters. A key finding is that

Table 1. Selected structural parameters of *S*-ethyl 4-chlorobenzoyl dithioester and *S*-ethyl 4-hydroxybenzoyl dithioester

Parameter	*S*-Ethyl 4-chlorobenzoate dithioester	*S*-Ethyl 4-hydroxybenzoate dithioester
Bond length/Å		
C═S	1.66	1.66
C—S	1.76	1.77
S—C	1.83	1.83
C—C_1	1.49	1.48
Ring C_iC_j	1.39–1.41	1.38–1.41
Cl—C_4	1.75	—
O—C_4	—	1.37
Bond angle/°		
S═C—S	124.4	123.7
C_1—C—S	112.7	112.9
C_1—C═S	122.9	123.3
C—S—CH_2	104.1	104.2
Dihedral angle/°		
S═C—C_1—C_6	32.4	28.3
S—C—C_1—C_2	33.9	30.0
S═C—S—CH_2	5.2	6.2
C_3—C_4—O—H	—	0.5

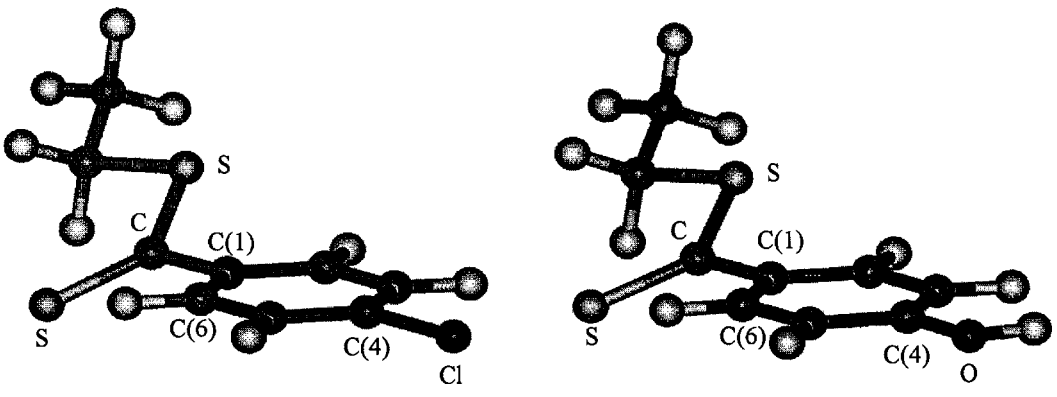

Figure 1. Geometry of the truncated substrate 4-CBA-dithio-CoA (coenzyme A moiety replaced by ethyl-) (left) and truncated product 4-HBA-dithio-CoA (coenzyme A moiety replaced by ethyl-) (right) predicted by density functional theory and *ab initio* theory, showing that S═C—S and phenyl ring are not coplanar in stable conformers.

the most stable forms of the dithiobenzoyl moiety of the 4-chlorobenzoyl dithioester and 4-hydroxybenzoyl dithioester exhibit non-planar skew structures. In the substrate analog, the dihedral angle S═C—C_1—C_6 = 32.4° and the dihedral angle S═C—C_1—C_2 = 33.9°; whereas in the product, the dihedral angle S═C—C_1—C_6 = 28.3° and the dihedral angle S═C—C_1—C_2 = 30.0°. Hence the S═C—S group is not coplanar with the benzene ring, implying reduced conjugation between the S═C and the ring.

The modestly distorted S═C—C—C angles found here are in keeping with those found for other dithioesters. Aliphatic dithioesters such as $CH_3CH_2C(=S)SCH_3$ and $CH_3CH_2C(=S)SCH_2CH_3$ do not adopt a planar skeleton as the most stable conformers. Instead, a skew form with a C—C—C═S dihedral angle equal to 100° is more stable than the symmetric *syn* conformer with a C—C—C═S dihedral angle equal to zero.[15] X-ray crystallographic analyses of six *N*-acylglycine ethyl dithioesters [including *N*-acetylglycine, *N*-(*β*-phenylpropionyl)glycine, *N*-benzoylglycine (two forms), *N*-(*p*-methylbenzoyl)glycine and *N*-(*p*-chlorobenzoyl)glycine ethyl dithioester] showed that the corresponding dihedral angle N—C—C═S ranges from −22.2° to +9.5° rather than keeping strictly to zero.[16] Thus, previous investigations by x-ray crystallographic analysis and quantum mechanics, and also by ^{13}C NMR studies,[17,18] illustrated that a restricted rotation along (C—)C—C(═S) (a non-zero dihedral angle for C—C—C═S) can occur in stable conformers of dithioesters. This contrasts with the situation for dioxy- or thioester analog [—C(O)O— and —C(O)S—], where planar skeletons are the norm.[19] For example, in the oxythioesters *S*-ethyl 4-chlorobenzoyl thiolester and *S*-ethyl 4-hydroxybenzoyl thiolester (either protonated or deprotonated forms), the O═C—C—C(6) dihedral angles are found to be zero.[8,9] This latter observation also suggests that the non-planarity observed for the dithio analogs in Fig. 1 is not due to steric hindrance involving the hydrogen atoms on C(6) or C(2). In essence, the dithioester analogs provide us with a unique opportunity to compare the effects of the electrostatic forces applied through the C═O or C═S group of the ligands on the benzoyl ring in the active site.

Raman spectra of *S*-ethyl 4-chlorobenzoate dithioester and *S*-ethyl 4-hydroxybenzoate dithioester and the corresponding CoA derivatives

The Raman spectrum of the free substrate 4-CBA-dithio-CoA (in aqueous solution, at pH 7.5) is shown in Fig. 2(A). Normal mode analysis of the truncated model *S*-ethyl 4-chlorobenzoate dithioester (where the large CoA moiety is substituted by an ethyl group, see Fig. 1, left) has been performed, based on both density functional and *ab initio* SCF theory, in order to assign the observed bands of the parent compound. A full list of the vibrational bands of the fingerprint region is given in Table 2, where a comparison is made to the corresponding modes in the parent CoA compound. The calculated results are very consistent with empirical assignments. Therefore, almost all of the Raman bands in Fig. 2(A) can be assigned, based on the calculations on the truncated form and with the help of Raman data for CoA, adenosine and ADP collected separately under similar conditions (unpublished work, this laboratory). The strong ring modes which appear in Fig. 2(A)

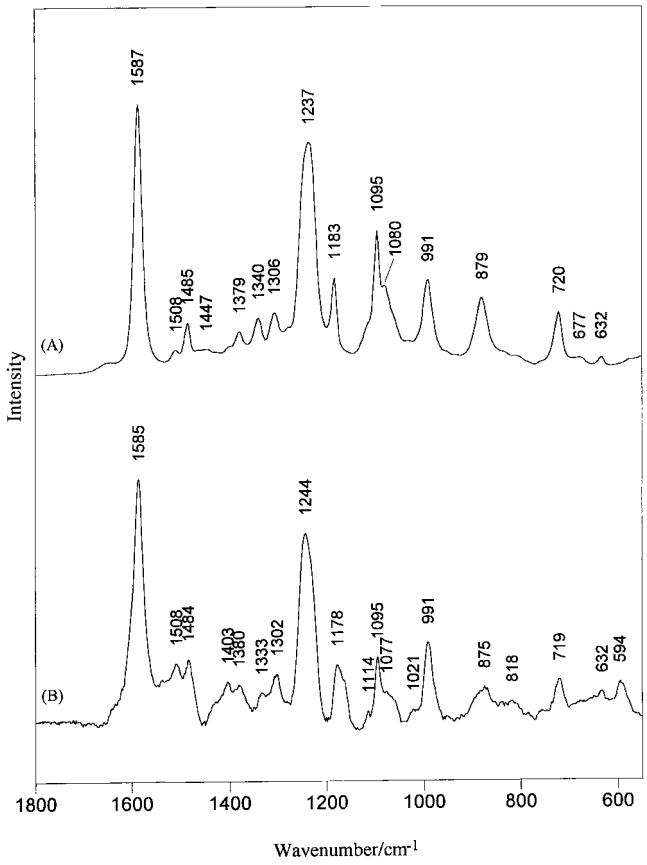

Figure 2. Raman spectra of substrate 4-chlorobenzoyl CoA dithioester (4-CBA-CoA dithioester) (A) free state, 8.8 mM in 50 mM Tris–HCl buffer, pH 7.5, data accumulation time 5 min; (B) bound to WT dehalogenase (180 μM in Tris–HCl buffer, pH 7.5) at the first minute.

at 1587, 1237 and 1183 cm^{-1} are characteristic of *para*-disubstituted benzenes. The first is an 8a,b mode (ring C═C stretching, in Wilson's notation, used hereafter; see Refs 13 and 14). The second at 1237 cm^{-1} is 7a′ and is a ring X-sensitive mode that involves C(1)–C(SS) stretching, C–H in-plane bending and a S═C–S symmetric stretching motion; its broad shape may be caused by torsions of the S═C–S group relative to the ring giving rise to a distribution of torsional angles. The 1183 cm^{-1} feature is a 9a mode consisting of ring C–H in-plane bending. The strong band at 1095 cm^{-1} is due to an X-sensitive mode (7a), involving C(4)–Cl stretching and ring C–H in-plane bending. An important point is that vibrational modes related to the S═C–S group are not localized; instead, they are highly coupled with adjacent ring modes that possess similar vibrational transition energies. This contrasts with oxy-esters (O═C—O or O═C—S), where the C═O stretching is often an approximate group wavenumber. Here, C═S stretching is mixed with a ring in-plane bending mode (18a) at 991 cm^{-1} and another ring mode (7a′ mode) at 1237 cm^{-1}. Similarly, C–S stretching is mixed with both a ring breathing mode (mode 1) that is observed at 879 cm^{-1}, and a ring in-plane mode (mode 13) that is observed at 720 cm^{-1}. The weak band at 677 cm^{-1} is due to S–C stretching coupled to CH_3 rocking, while the neighboring weak band at 632 cm^{-1} is due to a ring in-plane bending mode (Table 2). Other medium-to-weak bands in Fig. 2(A) are due to CoA adenine bands (1508, 1379, 1340 and 1306 cm^{-1}) or other CoA bands (e.g. the

Table 2. Density functional theory predicted normal modes and their wavenumbers ($\tilde{\nu}$) of *S*-ethyl 4-chlorobenzoate dithioester

$\tilde{\nu}$/cm^{-1}	Raman activity	Normal modes	Observed in water $\tilde{\nu}$/cm^{-1}
1595.1	376	Ring quadrant stretch (8a)	1587 s
1566.1	1	Ring quadrant stretch (8b)	
1488.6	22	Ring semicircle stretch (19a)	1485 m
1488.2	7	CH_3 asym. bend	
1482.6	16	CH_3 asym. bend	
1455.5	10	CH_2 scissor	1447 w
1404.1	2	CH_3 sym. bend	
1402.9	1	Ring semicircle stretch (19b)	
1303.2	2	Ring mode 3: ring C–H in-plane bend + ring C(4)–OH bend	
1301.6	0	Ring ν 14 : ring C–H in-plane bend	
1282.8	4	CH_2 wag	1278 w
1237.4	6	CH_2 twist	
1226.4	323	Ring X-sensitive mode 7a′ : C(1)–C stretch + ring C–H in-plane bend + C=S stretch	1237 s
1186.6	32	Ring C–H in-plane bend (ν 9a)	1183 s
1122.7	0	Ring C–H in-plane bend (ν 15)	
1083.6	46	Ring X-sensitive mode 7a : C(4)–Cl stretch + ring C–H in-plane bend	1095 s
1060.4	10	CH_3 rock + CH_2 twist	
1039.7	3	CH_2 twist + CH_3 rock	1032 w
1027.2	20	C=S stretch + ring mode 18a + CH_3 bend	991 s
1002.2	3	ν 18a : ring in-plane bend + ring C–H in-plane bend	
969.9	10	C–C stretch in ethyl	
959.9	2	Ring C–H out-of-plane bend (ν 17a)	
948.4	0	Ring C–H out-of-plane bend (ν 5)	
870.4	6	Ring breathing (ν 1) + C–S stretch	879 s
824.9	3	Ring C–H out-of-plane bend (ν 11)	
815.4	3	Ring C–H out-of-plane bend (ν 10a)	
772.1	0	CH_2 rock + CH_3 rock	
707.8	12	Ring in-plane bend (ν 13) + C–S stretch	720 s
705.0	3	Ring out-of-plane bend (ν 4)	
665.4	49	S–C stretch + CH_3 rock	677 w
627.7	6	Ring in-plane bend (ν 6b)	632 w
572.6	2	Ring out-of-plane bend (ν 16b)	
513.5	4	S=C–S sym. stretch + ring in-plane bend (ν 13) + S=C–S out-of-plane bend	518 m
476.4	1	Ring out-of-plane bend (ν 16b′)	
417.3	2	Ring in-plane bend (6a) + S=C–S scissor + C–S–C scissor	410 m
407.8	2	Ring out-of-plane bend (16a)	
378.5	3	Ring in-plane bend (9b) + ring out-of-plane bend (10b)	
307.5	2	Ring in-plane bend (18b) + CH_3 torsion	

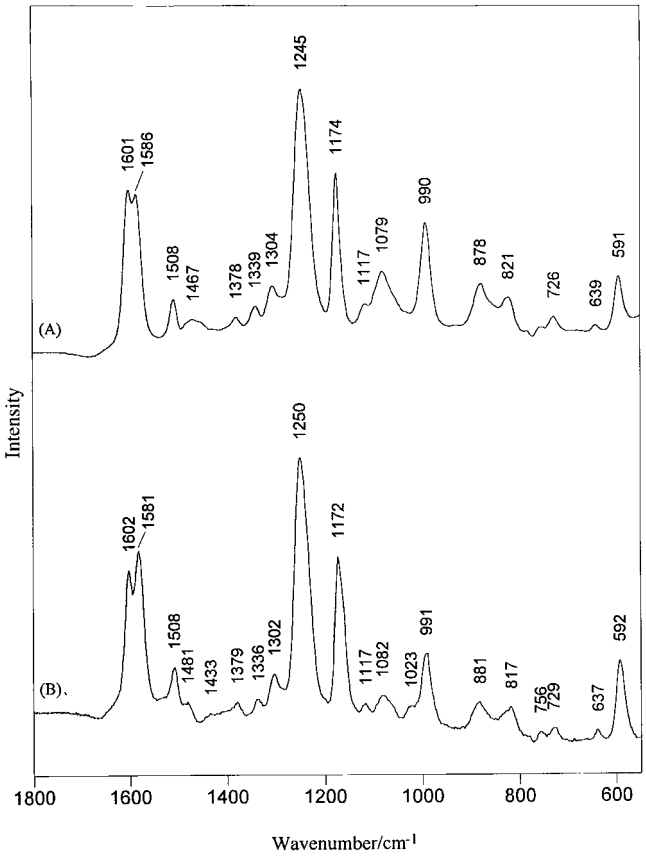

Figure 3. Raman spectra of product 4-hydroxybenzoyl CoA dithioester (4-HBA-CoA dithioester): (A) free state, 2.0 mM in 50 mM Tris–HCl buffer, pH 7.5, data accumulation time 5 min; (B) bound to WT dehalogenase (180 μM in 50 mM Tris–HCl buffer, pH 7.5), data accumulation time 5 min.

1080 cm^{-1} feature from CoA's diphosphate moiety) or overlapping bands (1485 cm^{-1}) from CoA and benzoyl ring moieties.

The spectrum of free product 4-HBA-dithio-CoA [Fig. 3(A)] shows typical phenyl ring modes at 1601, 1586 cm^{-1} (8a and 8b modes), 1245 (7a′ mode) and 1174 cm^{-1} (9a mode), and also CoA features which are almost the same as in the substrate analog [Fig. 2(A)]. The results of normal mode analysis of the truncated product (Fig. 1, right) provide additional insight and Table 3 lists the normal modes in the fingerprint region predicted by DFT. The results are found to be consistent with conventional assignments. Again, Raman bands related to the S=C—S group are found to be coupled with ring modes; as for the substrate analog, the C=S stretching mode is coupled with a ring in-plane bending mode (18a mode) at 990 cm^{-1} and another ring mode, 7a′, at 1245 cm^{-1}. The C–S stretching is mixed with both the ring breathing (mode 1) (observed at 878 cm^{-1}) and the ring in-plane bending mode (mode 13), the latter is seen at 821 cm^{-1} in contrast to the analogous feature at 722 cm^{-1} in the substrate. A strong band at 591 cm^{-1} is due to S=C—S symmetric stretching coupled with S=C—S out-of-plane bending and a ring in-plane bending and does not have an analogue in the substrate. The features at 1508 and 639 cm^{-1} (Fig. 3) are ring modes (Table 3), while the peak at 726 cm^{-1} is an adenine ring mode from the CoA moiety.

Raman spectra of substrate, 4-CBA-dithio-CoA and product, 4-HBA-dithio-CoA, bound to the enzyme dehalogenase

Although the substrate, 4-CBA-dithio-CoA, binds avidly to dehalogenase with a K_m of 33 μM, the reaction proceeds slowly. The rate constant is 0.00323 s^{-1}, which means that the half-life of the Michaelis complex is 3–4 min before conversion to product occurs. Since the Raman data were collected with a 60 s acquisition time, it was possible to obtain Raman spectra before the majority of complexes

Table 3. Density functional theory predicted normal modes and their wavenumbers ($\tilde{\nu}$) of *S*-ethyl 4-hydroxybenzoate dithioester

$\tilde{\nu}$/cm^{-1}	Raman activity	Normal modes	Observed in water $\tilde{\nu}$/cm^{-1}
1612.2	418	Ring quadrant stretch (8a)	1601 s
1585.8	20	Ring quadrant stretch (8b)	1586 s
1507.7	36	Ring semicircle stretch (19a)	1508 m
1486.9	7	CH_3 asym. bend	
1480.9	15	CH_3 asym. bend	
1455.2	10	CH_2 scissor	1467 w
1435.0	1	Ring semicircle stretch (19b)	
1401.9	2	CH_3 sym. bend	
1346.0	3	Ring mode 3: ring C–H in-plane bend + ring C(4)–OH bend	
1305.9	102	Ring ν 14: ring C–H in-plane bend	1304 m
1281.5	4	CH_2 wag	
1270.9	7	Ring X-sensitive mode 7a: C(4)–O stretch + ring C–H in-plane bend	
1236.1	6	CH_2 twist + CH_3 rock	
1231.5	320	Ring X-sensitive mode 7a′: C(1)–C stretch + ring C–H in-plane bend + C=S stretch	1245 s
1178.0	133	Ring C–H in-plane bend (ν 9a)	1174 s
1165.6	10	O–H in-plane bend	
1117.5	7	Ring C–H in-plane bend (ν 15)	
1058.5	4	CH_3 rock + CH_2 twist	
1038.2	3	CH_2 twist + CH_3 rock	
1021.6	25	C=S stretch + ring mode 18a + CH_3 bend	990 s
1000.6	1	ν 18a: ring in-plane bend + ring C–H in-plane bend	
969.2	10	C–C stretch in ethyl	
960.6	6	Ring C–H out-of-plane bend (ν 17a)	
932.0	0	Ring C–H out-of-plane bend (ν 5)	
870.5	10	Ring breathing (ν 1) + C–S stretch	878 m
832.4	4	Ring C–H out-of-plane bend (ν 11)	
806.3	39	Ring in-plane bend (ν 13) + C–S stretch	821 m
794.0	2	Ring C–H out-of-plane bend (ν 10a)	
772.3	0	CH_2rock + CH_3 rock	
707.2	4	Ring out-of-plane bend (ν 4)	
670.1	28	S–C stretch + CH_3 rock	
634.5	6	Ring in-plane bend (ν 6b)	639 w
582.5	10	S=C–S sym. stretch + ring in-plane bend (ν 13) + S=C–S out-of-plane bend	591 m
571.8	5	Ring out-of-plane bend (ν 16b)	
492.1	2	Ring out-of-plane bend (ν 16b′)	
449.3	4	Ring in-plane bend (6a) + S=C–S scissor + C–S–C scissor	438 w
421.4	1	Ring in-plane bend (9b)	
411.3	3	Ring out-of-plane bend (16a)	412 w
374.2	2	O–H out-of-plane bend	
360.7	3	Ring in-plane bend (10b)	

converted from substrate to product. Figure 2 compares the Raman difference spectrum of free substrate, 4-CBA-dithio-CoA, with that of the substrate in the active site of dehalogenase. In the latter, the shoulders near 1170 and 820 cm^{-1} and the peak at 594 cm^{-1} are due to the presence of product, this being formed during the time it took to record the Raman spectrum. However, substrate peaks still dominate the spectrum. In addition, there may be small contributions from enzyme modes that do not subtract to zero in the Raman difference experiment because the protein undergoes a conformational change upon ligand binding. The band at 1403 cm^{-1} in Fig. 2 may be such a feature, since it is seen in the Raman difference spectra of many dehalogenase complexes;[6,8,9] however, its origin is not fully understood.

Overall, in Fig. 2 the spectrum of the bound substrate resembles closely that of the free molecule. The peaks involving C=S coupled to ring modes near 1240 and 991 cm^{-1} are little perturbed, and the C—S modes (coupled to ring motions), near 879 and 720 cm^{-1}, show, at most, some broadening. We make the assumption that the conformation about the dithioester bonds is the same for the model compound seen in Fig. 1 and the parent CoA compound. Thus the Raman results suggest that the conformation about the dithioester–phenyl linkages remains essentially unchanged upon binding and is close to that seen in Fig. 1. The feature near 1095 cm^{-1} that contains a major contribution from 4-Cl-phenyl stretch is also unchanged for the bound substrate and this indicates that this Cl—C bond is not strongly perturbed in the active site. The pattern of the adenine triplet, the 1306, 1340 and 1379 cm^{-1} bands, changes upon binding with the 1340 cm^{-1} peak, shifting down and losing its relative intensity. Similar changes are seen for other substrate analog–CoA ligands binding to dehalogenase and undoubtedly represent changes in the hydrogen bonding pattern around the adenine ring as it leaves an aqueous environment and binds to the protein.[5,8]

Figure 3 compares the product, 4-HBA-dithio-CoA, in its free and enzyme-bound forms. As for the substrate there is no evidence for major spectroscopic changes upon binding. One of the most significant differences between the two spectra in Fig. 3 is the modest intensity increase of the ring C=C stretching mode seen at 1581 cm^{-1}; however, the positions of the 8a and 8b modes do not change markedly. The band at the 1245 cm^{-1} 7a′ mode undergoes a small shift to 1250 cm^{-1}, whereas the band at 1174 cm^{-1} (9a mode), with no contribution from vibrations of the dithioester group, has hardly shifted. In addition, the band near 1079 cm^{-1} has diminished its intensity upon binding. This band is from the phosphate linkages that are part of the CoA molecule and this functionality must therefore be perturbed on going from aqueous solution to the active site. The most remarkable fact about the spectrum of the bound product is that it resembles so closely the spectrum of the free product. This is in stark contrast to the true product, which only differs by the C=S in the present system being replaced by C=O, where the Raman spectrum undergoes radical changes upon binding.[5] For example, the characteristic 8a, 8b benzene ring modes are seen at 1601 and 1586 cm^{-1} in the free (C=O) product, but upon binding they are replaced by bands at 1560 and 1525 cm^{-1}; while the band at 1171 cm^{-1} (ring 9a mode, C–H in-plane bending) undergoes a drastic reduction in intensity. This is due to major π-electron reorganization with the benzoyl system becoming quinonoid-like in the active site. As shown in Scheme 2, contributions from canonical form **II** become much more prevalent in the active site.

The highly polarized π-electron system seen in the bound product also gives rise to a large red shift in the absorption spectrum upon binding. For the natural form of the product the λ_{max} shifts from 294 to 371 nm. For the dithio analog the λ_{max} (at 338 nm) does not shift upon binding, indicating that neither the dithioester nor the substituted phenyl group undergoes detectable changes

in their electronic states (note that both the dithioester and the phenyl ring are chromophores). The Raman data therefore show unambiguously that the dithioester analog retains its benzenoid character and there is no evidence for any perturbation to the π-electrons. There is a firm molecular model for the causes of electron reorganization in the case of the natural (C═O) product; this is outlined in the Introduction and can be used to explore why the dithio analog is so different. Although an x-ray crystal structure is not available for the complex with the dithio analog of 4-HBA-CoA, it is most likely resembles closely that seen in Scheme 2. The reason why electron polarization does not occur in the dithio–ligand complex must reside in the different properties of C═O and C–S. The latter is a poorer hydrogen bond acceptor,[20] and the sulfur atom is larger than oxygen (with a van der Waals radius of 1.85 Å for the former and 1.40 Å for the latter[21]). The C═S bond, 1.66 Å, is also considerably longer than the C═O bond, 1.22 Å. These factors mean that the C═S group will not fit as comfortably, either sterically or energetically, into the 'positive hole' for C═O that Nature has designed in the active site. This will result in less electron pull at the C═S sulfur atom. Moreover, the sulfur atom, as a result of its larger size, is more poorly conjugated with the phenyl ring and this effect is exacerbated by the non-planarity of the dithiophenyl system discussed above. The net result of these factors is that electron pull at the C═S is ineffective and the benzoyl's π-electrons are unperturbed.

The lack of electron pull, that can be transmitted throughout the benzoyl's electrons, has serious catalytic consequences. This results from the fact that the electron pull at the C═O group is an important part of the catalytic mechanism, that is used to reduce electron density at the 4-position and thus facilitate the Cl atom replacement by OH. This is why the dithio analog is a much slower substrate, by a factor of $\sim$200, than the natural substrate; k_{cat} for the latter is 0.6 s^{-1} and that for the former is 0.00323 s^{-1}.

Acknowledgments

The authors are grateful to the Ohio Supercomputer Center for computational facilities (project PDS 183). This work was supported by the NIH, grants GM-54072 (to P.R.C.) and GM-28688 (to D.D.M.).

REFERENCES

1. Scholten JD, Chang K-H, Babbitt PC, Charest H, Sylvetre M, Dunaway-Mariano D. *Science* 1991; **253**: 182.
2. Chang KH, Liang P-H, Beck W, Scholten JD, Dunaway-Mariano D. *Biochemistry* 1992; **31**: 5605.
3. Liang P-H, Yang G, Dunaway-Mariano D. *Biochemistry* 1993; **32**: 12245.
4. Benning MM, Taylor KL, Liu R, Yang G, Xiang H, Wesenberg G, Dunaway-Mariano D, Holden HM. *Biochemistry* 1996; **35**: 8103.
5. Taylor KL, Liu R, Liang P-H, Price J, Dunaway-Mariano D, Tonge PJ, Clarkson J, Carey PR. *Biochemistry* 1995; **34**: 13881.
6. Clarkson J, Tonge PJ, Taylor KL, Dunaway-Mariano D, Carey PR. *Biochemistry* 1997; **36**: 10192.
7. Dong J, Dinankarpandian D, Carey PR. *Appl. Spectrosc.* 1998; **52**: 1117.
8. Dong J, Xiang H, Luo L, Dunaway-Mariano D, Carey PR. *Biochemistry* 1999; **38**: 4198.
9. Xiang H, Dong J, Carey PR, Dunaway-Mariano D. *Biochemistry* 1999; **38**: 4207.
10. Liang P-H. PhD Thesis, University of Maryland, College Park, MD, 1994; 166.
11. Frisch MJ, Trucks GW, Schlegel HB, Gill PMW, Johnson BG, Robb MA, Cheeseman JR, Keith T, Petersson GA, Montgomery JA, Raghavachari K, Al-Laham MA, Zakrzewski VG, Ortiz JV, Foresman JB, Cioslowski J, Stefanov BB, Nanayakkara A, Challacombe M, Peng CY, Ayala PY, Chen W, Wong MW, Andres JL, Replogle ES, Gomperts R, Martin RL, Fox DJ, Binkley JS, Defrees DJ, Baker J, Stewart JP, Head-Gordon M, Gonzalez C, Pople JA. *Gaussian 94, Revision E.2*. Gaussian: Pittsburgh, PA, 1995.
12. Becke AD. *J. Chem. Phys.* 1993; **98**: 5648.
13. Colthup NB, Daly LH, Wiberly SE. *Introduction to Infrared and Raman Spectroscopy* (2nd edn). Academic Press: New York, 1975.
14. Dollish FR, Fateley WG, Bentley FF. In *Characteristic Raman Frequencies of Organic Compounds*. John Wiley & Sons: New York, 1973; 175.
15. Fausto R, Martins AG, Teixeira-Dias JJC, Tonge PJ, Carey PR. *J. Phys. Chem.* 1994; **98**: 3592.
16. Kim M, Birnbaum GI, Hynes RC, Neugebauer W, Carey PR. *J. Am. Chem. Soc.* 1993; **115**: 6230.
17. Brouwer AC, Bos HJT. *Recl. Trav. Chim. Pays-Bas* 1983; **102**: 103.
18. Fischer H, Treier K, Troll C. *Chem. Ber.* 1995; **128**: 883.
19. Fausto R, Tonge PJ, Carey PR. *J. Chem. Soc., Faraday Trans.* 1994; **90**: 3491.
20. Laurence C, Berthelot M, Lequestel JY, Elghomari MJ. *J. Chem. Soc., Perkin Trans. 2* 1995; 2075.
21. Cotton FA, Wilkinson G. *Advanced Inorganic Chemistry, a Comprehensive Text*. Interscience: London, 1962; 104.

